3

Summer-Time Rainfall Variability in the Tropical Atlantic

Guojun Gu
Earth System Science Interdisciplinary Center,
University of Maryland, College Park, MD
& Laboratory for Atmospheres,
NASA Goddard Space Flight Center, Greenbelt, MD
U.S.A.

1. Introduction

Convection and rainfall in the tropical Atlantic basin exhibit intense variations on various time scales (e.g., Nobre & Shukla, 1996; Giannini et al., 2001; Chiang et al., 2002). The Atlantic Intertropical Convergence Zone (ITCZ) stays always north of the equator with the trade winds converging into it, representing a prominent climate feature on the seasonal time scale. The ITCZ, though generally over the open ocean, extends to the northeast coast of South America during boreal spring and to the West African continent during boreal summer. Longer-than-seasonal time scale variability is also evident and has been extensively explored in the past through both observational analyses and modeling studies (*e.g.,* Lamb, 1978a, b; Carton & Huang, 1994; Nobre & Shukla, 1996; Sutton et al., 2000). The Atlantic Niño and an interhemispheric sea surface temperature (SST) gradient mode are discovered to be the two major local forcing mechanisms (*e.g.,* Zebiak, 1993; Nobre & Shukla, 1996), in addition to the two other remote large-scale forcings: the El Niño-Southern Oscillation (ENSO) and the North Atlantic Oscillation (NAO) (*e.g.,* Curtis & Hastenrath, 1995; Chiang et al., 2002; Wang, 2002). The most intense year-to-year variability in the tropical Atlantic is usually observed during boreal spring [March-April-May (MAM)], specifically in the western basin and over the northeastern portion of South America, when the marine ITCZ approaches the equator (*e.g.,* Hastenrath & Greischar, 1993; Nobre & Shukla, 1996). Therefore, most of past studies have been primarily focused on this season (*e.g.,* Chiang et al., 2002; Gu & Adler, 2006).

Intense interannual variability has also been seen during boreal summer [June-July-August (JJA)] in the tropical Atlantic (e.g. Sutton et al., 2000; Gu & Adler, 2006, 2009). The Atlantic Niño becomes mature during this season, and the impact of the interhemispheric SST gradient mode and ENSO can still be felt in the equatorial region (*e.g.,* Sutton et al., 2000; Chiang et al., 2002). Particularly, evident interannual variations exist in various distinct severe weather phenomena such as African easterly waves (AEW) and associated convection, and Atlantic hurricane activity (*e.g.,* Thorncroft & Rowell, 1998; Landsea et al., 1999). These severe weather systems frequently appear during boreal summer and fall, and

usually propagate westward near the latitudes of the ITCZ (*e.g.,* Chen & Ogura, 1982; Gu & Zhang, 2001).

Hence, based on the two recent studies (Gu & Adler, 2006, 2009), summer-time rainfall variations within the tropical Atlantic basin are further explored here with a focus on the effects of two local SST modes and ENSO. The global monthly precipitation information from the Global Precipitation Climatology Project (GPCP) is applied (Adler et al., 2003). On a global 2.5°×2.5° grid, this satellite-based product is combined from various data sources: the infrared (IR) rainfall estimates from geostationary and polar-orbiting satellites, the microwave estimates from Special Sensor Microwave/Imager (SSM/I), and surface rain gauges from the Global Precipitation Climatological Centre (GPCC) in Germany. The global SST anomalies and three climatic modes are computed using a satellite-based SST product from the National Centers for Environmental Prediction (NCEP) (Reynolds et al., 2002). This product, archived on 1°×1° grids, is built through recons-spatial interpolation, and lasts from January 1982 to present. The results shown here are focused on the time period of January 1982-December 2006. Additionally, monthly surface wind anomalies are derived using the products from the National Centers for Environmental Prediction (NCEP) and National Center for Atmospheric Research (NCAR) reanalysis project (Kalnay et al., 1996). All monthly anomalies, and rainfall and SST indices constructed here are de-trended as we primarily focus on the variations on the interannual time scale.

2. Seasonal-mean rainfall and SST variations during JJA and MAM

Detailed seasonal variations in the tropical Atlantic have been examined in past studies (*e.g.,* Mitchell & Wallace, 1992; Biasutti et al., 2004; Gu & Adler, 2004). Here we just give a brief summary of seasonal-mean features of rainfall and SST, and their corresponding interannual variances during JJA and MAM (Fig. 1). Seasonal-mean oceanic rainfall generally stays over warm SST (≥27°C), featuring the climatological state of the ITCZ. The marine rainfall band is also closely connected to the rainfall zones over the two neighboring continents. During MAM (Fig. 1c), the most intense rainfall zone is located over the coastal region of the northeastern South America; simultaneously the oceanic rainfall band or the marine ITCZ approaches the equator, following the warmest SST in the equatorial region due to the relaxation of trade winds particularly in the eastern basin. During JJA (Fig. 1a), an equatorial cold tongue-ITCZ complex forms with the maritime ITCZ becoming strongest and moving to the north, with two rainfall zones concomitantly being seen over the northern South America and West Africa, respectively.

During MAM (Fig. 1d), the most intense rainfall variability occurs in the western equatorial region, especially along the coastline. In contrast, the maximum SST variances are generally observed in the eastern basin, and are generally concentrated in three areas: tropical north Atlantic (~5°-25°N), the equatorial region, and tropical south Atlantic (~10°-25°S). Furthermore, the most intense SST variability tends to be away from the equator, with thus a much weaker SST variability along the equator. During JJA (Fig. 1b), rainfall variances are mostly found to be over the open ocean along the mean latitudes of the ITCZ. Major SST variability is located in the equatorial region, corresponding to the frequent appearance of the Atlantic Niño (*e.g.,* Zebiak, 1993; Carton & Huang, 1994). Interestingly, rainfall variances within the interior of two continents, particularly over West Africa, are much weaker compared with over ocean and in the coastal zone.

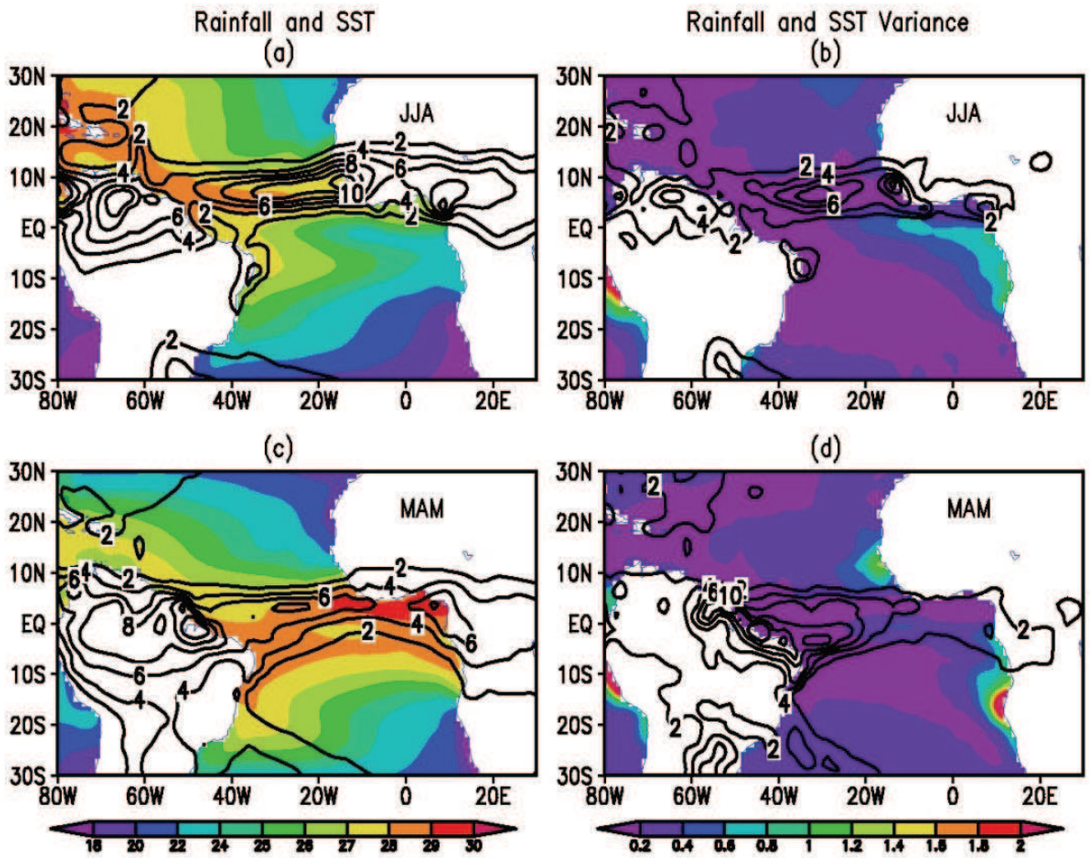

Fig. 1. Seasonal mean rainfall (*mm day*$^{-1}$; contours) and SST (^{o}C; color shades) during (a) June-August (JJA) and (c) March-May (MAM); Seasonal mean variances of rainfall (*mm*^{2} *day*$^{-2}$; contours) and SST [(^{o}C)^{2}; color shades] during (b) JJA and (d) MAM.

3. Spatial structures of SST anomalies associated with rainfall variations in the tropical Atlantic

To quantitatively investigate rainfall variability, two indices are defined to represent the strength (P_{ITCZ}) and latitude (Lat_{ITCZ}) variations of the marine ITCZ, respectively, with another one denoting the rainfall variability within the entire tropical Atlantic basin (P_{dm}). The tropical (25^{o}S-25^{o}N) meridional rainfall peak ($P_{max}(j)$, here j is an index of latitude) of monthly rainfall averaged along the longitudinal band of 15^{o}-35^{o}W, is determined for each month, including its latitude ($Lat_{max}(j)$). Then, this maximum rainfall value ($P_{max}(j)$) is weighted by the ones at the two neighboring latitudes (P(j-1) and P(j+1)) to yield a relatively smoother value for the ITCZ strength (P_{ITCZ}). The ITCZ latitude (Lat_{ITCZ}) is then estimated based on $Lat_{max}(j)$ and its two neighboring latitudes (Lat(j-1) and Lat(j+1)) weighted by their corresponding rainfall values. The resulting ITCZ latitude (Lat_{ITCZ}) thus depends on all these three rainfall values. The GPCP monthly rainfall product has a coarse (2.5^{o}×2.5^{o}) spatial resolution. This interpolation method can provide a relatively smooth (and reasonable), latitudinal change of the ITCZ north-south migration. The resultant ITCZ latitudes are in general confirmed by derived from both the similar NOAA/NCEP-CMAP

satellite-based monthly precipitation product and a merged, short-record (1998-2006) 1°×1° TRMM (3B43) monthly rainfall product (not shown). The basin-mean rainfall is computed over a domain of 15°S-22.5°N, 15°-35°W. Finally, P_{ITCZ}, Lat_{ITCZ}, and P_{dm} are determined by subtracting their corresponding mean seasonal cycles.

Time series for these three indices are depicted in Fig. 2. Rainfall changes during these two seasons are comparable calibrated by either P_{ITCZ} or P_{dm}. However, the ITCZ does not change much its mean latitudes during JJA, in contrast to evident fluctuations during MAM. Thus the major rainfall changes during JJA are related to the variability of the ITCZ strength and/or the basin-mean rainfall. This probably implies a lack of forcing mechanism on the ITCZ location during JJA. Past studies suggested that the Atlantic interhemispheric SST mode, though a dominant factor of the ITCZ position during MAM, becomes secondary during JJA (*e.g.,* Sutton et al., 2000; Gu & Adler, 2006).

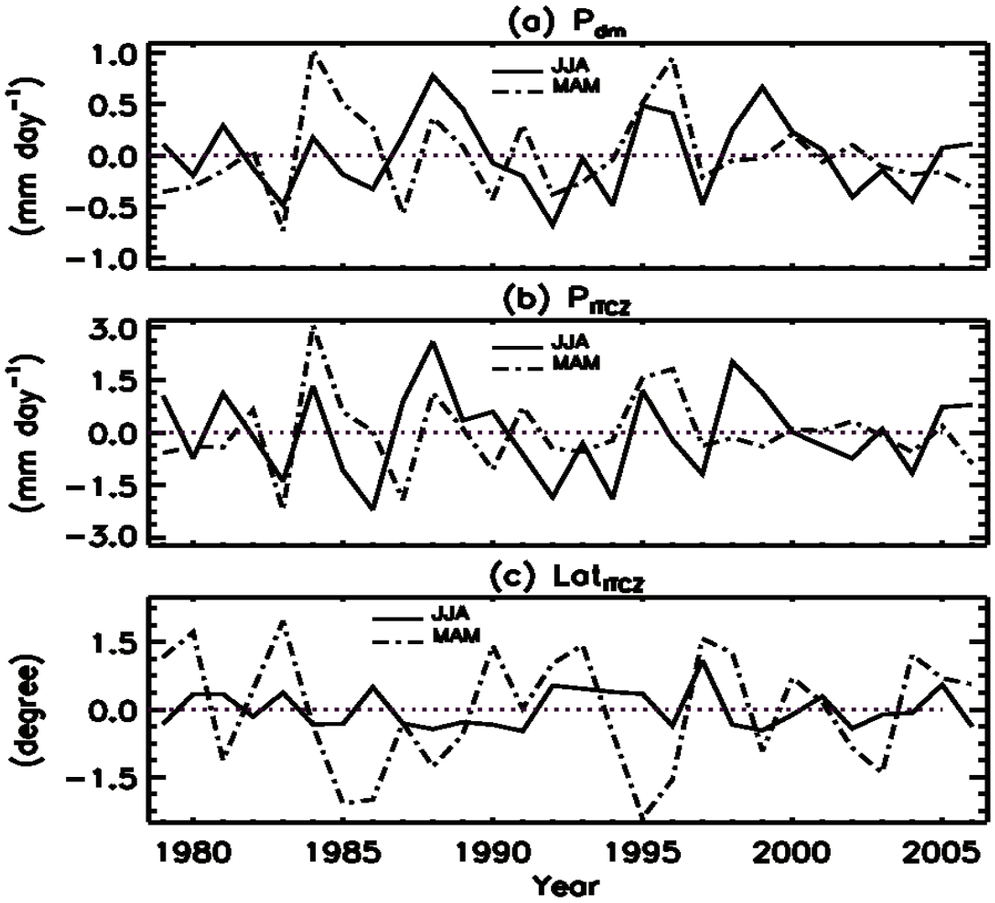

Fig. 2. Time series of (a) the domain-mean rainfall (P_{dm}), (b) the ITCZ strength (P_{ITCZ}), and (c) the ITCZ latitudes (Lat_{ITCZ}) during JJA (solid) and MAM (dash-dot).

Simultaneous correlations between SST anomalies with P_{ITCZ} and Lat_{ITCZ} are estimated during both seasons (Fig. 3). During JJA, the major high-correlation area of SST anomalies with P_{ITCZ} is located west of about 120°W in the tropical central-eastern Pacific, and the correlations between SST anomalies and Lat_{ITCZ} are generally weak in the tropical Pacific. Within the tropical Atlantic, significant, positive correlations with P_{ITCZ} roughly cover the

entire basin from 20°S to 20°N. It is of interest to note that the same sign correlation is found both north and south of the equator, suggesting a coherent, local forcing of rainfall variability during JJA. Furthermore, evident negative correlations between SST anomalies and Lat_{ITCZ} are seen within the deep tropics especially along and south of the equator. These confirm the weakening effect of the interhemispheric SST gradient mode during JJA (e.g., Sutton et al., 2000).

During MAM, the ITCZ strength is strongly correlated to SST anomalies in both the equatorial Pacific and Atlantic (e.g., Nobre & Shukla, 1996; Sutton et al., 2000; Chiang et al., 2002). However, the significant negative correlations tend to appear along the equator in the central-eastern equatorial Pacific (east of 180°W) and along the western coast of South America, quite different than during JJA. Roughly similar correlation patterns can also be observed for Lat_{ITCZ} in the tropical Pacific. Within the tropical Atlantic basin, P_{ITCZ} tends to be correlated with SST anomalies along and south of the equator, but the high correlation area shrinks into a much smaller one compared with that during JJA. The lack of high (negative) correlation north of the equator further confirms that the interhemispheric SST mode strongly impacts the ITCZ locations (Fig. 3d), but has a minor effect on the ITCZ strength (*e.g.,* Nobre & Shukla, 1996).

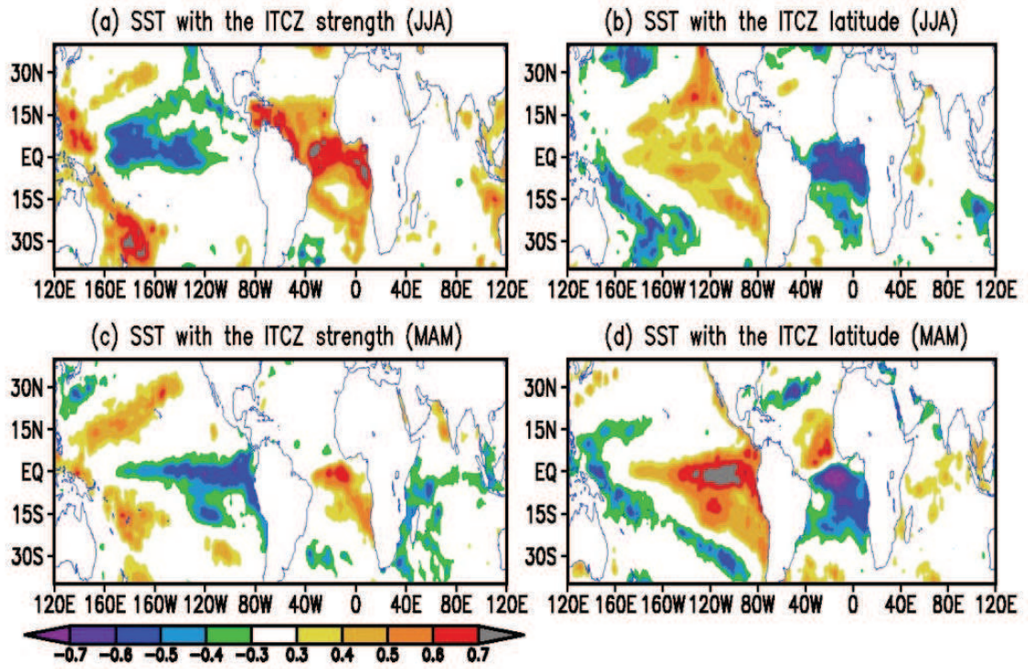

Fig. 3. Correlations of SST anomalies with (a, c) the ITCZ strength (P_{ITCZ}) and (b, d) the ITCZ latitude (Lat_{ITCZ}) during (a, b) MAM and (c, d) JJA. The 5% significance level is ±0.4 based on 23 degrees of freedom (*dof*s).

During these two seasons there are also two major large areas of high correlation for both P_{ITCZ} and Lat_{ITCZ} in the tropical western Pacific, though with different spatial features: One is along the South Pacific Convergence Zone (SPCZ), another is north of 10°N. These two features are probably associated with the ENSO effect and other factors, and not directly related to the changes in the tropical Atlantic, which are supported by weak regressed SST anomalies (not shown).

4. The effects of three major SST modes

To further explore the relationships between rainfall anomalies in the tropical Atlantic and SST variability, particularly during JJA, three major SST indices are constructed. Here, Nino3.4, the mean SST anomalies within a domain of 5°S-5°N, 120°-170°W, is as usual used to denote the interannual variability in the tropical Pacific. As in Gu & Adler (2006), the SST anomalies within 3°S-3°N, 0-20°W are defined as Atl3 to represent the Atlantic Equatorial Oscillation (*e.g.,* Zebiak, 1993; Carton & Huang, 1994). SST variability in the tropical north Atlantic is denoted by SST anomalies averaged within a domain of 5°-25°N, 15°-55°W (TNA). In addition, another index (TNA1) is constructed for comparison by SST anomalies averaged over a slightly smaller domain, 5°-20°N, 15°-55°W. We are not going to focus on the interhemispheric SST mode here because during boreal summer this mode becomes weak and does not impact much on the ITCZ (*e.g.,* Sutton et al., 2000; Gu & Adler, 2006), and the evident variability of the ITCZ is its strength rather than its preferred latitudes (Fig. 2). Same procedures are applied to surface zonal winds in the western basin (5°S-5°N, 25°-45°W) to construct a surface zonal wind index (U_{WAtl}).

As discovered in past studies (*e.g.,* Nobre & Shukla, 1996; Czaja, 2004), evident seasonal preferences exist in these indices (Fig. 4). ENSO usually peaks during boreal winter. The most intense variability in the tropical Atlantic appears during boreal spring and early summer. The maxima of both TNA and TNA1 are in April, about three months later than the strongest ENSO signals (*e.g.,* Curtis & Hastenrath, 1995; Nobre & Shukla, 1996). Surface zonal wind anomaly in the western equatorial region (U_{WAtl}) attains its maximum in May, followed by the most intense equatorial SST oscillation (Atl3) in June. Münnich & Neelin (2005) suggested that there seems a chain reaction during this time period in the equatorial Atlantic region. It is thus further arguable that the tropical western Atlantic (west of 20°W) is a critical region passing and/or inducing climatic anomalies in the equatorial Atlantic basin.

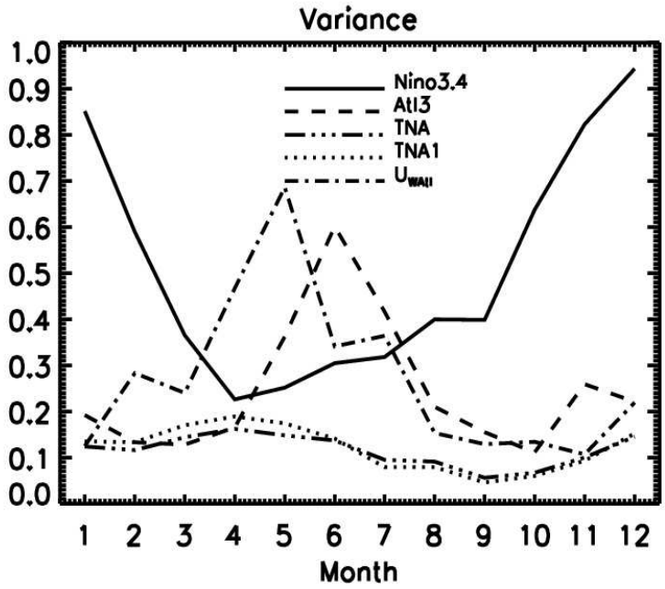

Fig. 4. Variances of various indices as a function of month. The variance of Nino 3.4 is scaled by 2.

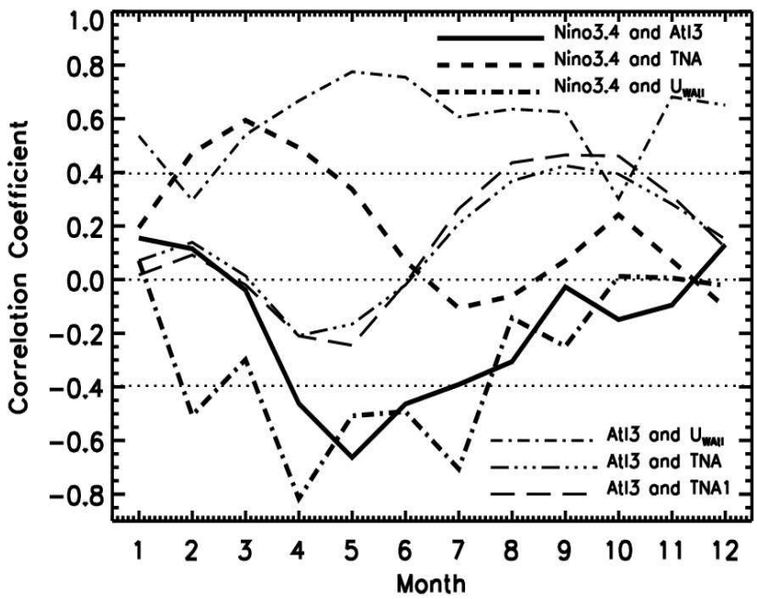

Fig. 5. Correlation coefficients between various indices as function of month. The 5% significance level is ±0.41 based on 21 dofs.

4.1 Relationships between various indices

Simultaneous correlations between SST indices are computed for each month (Fig. 5). The Pacific Niño shows strong impact on the tropical Atlantic indices. Significant correlations are found between Nino3.4 and TNA during February-April with a peak in March. The negative correlation between Nino3.4 and Atl3 becomes statistically significant during April-June, showing the impact of the ENSO on the Atlantic equatorial mode (*e.g.,* Delecluse et al., 1994; Latif & Grötzner, 2000). U_{WAtl} is consistently, negatively correlated with Nino3.4 during April-July except in June when the correlation coefficient is slightly lower than the 5% significance level. Interestingly, there are two peak months (April and July) for the correlation between U_{WAtl} and Nino3.4 as discovered in Münnich & Neelin (2005). High correlations between Atl3 and U_{WAtl} occur during March-July. These correlation relations tend to support that zonal wind anomalies at the surface in the western basin is a critical part of the connection between the equatorial Pacific and the equatorial Atlantic. Münnich & Neelin (2005) even showed a slightly stronger correlation relationship. Atl3 is also significantly correlated to U_{WAtl} in other several months, *i.e.,* January, September, and November, probably corresponding to the occasional appearance of the equatorial oscillation event during boreal fall and winter (*e.g.,* Wang, 2002; Gu & Adler, 2006).

Within the tropical Atlantic basin, the correlations between Atl3 and SST anomalies north of the equator (TNA and TNA1) become positive and strong during late boreal summer, particularly between Atl3 and TNA1 (above the 5% significance level during August-October). As shown in Fig. 4, SST variations north of the equator become weaker during boreal summer. Simultaneously the ITCZ and associated trade wind system move further to the north. It thus seems possible to feel impact in the TNA/TNA1 region from the equatorial region during this time period for surface wind anomalies-driven ocean transport (*e.g.,* Gill, 1982).

Lag-correlations between various SST indices are estimated to further our understanding of the likely, casual relationships among them (Figs. 6, 7, and 8). The base months for SST indices are chosen according to their respective peak months of variances (Fig. 4). The strongest correlation between Atl3 in June and Nino3.4 is found when Nino3.4 leads Atl3 by one month (Fig. 6), further confirming the remote forcing of ENSO on the Atlantic equatorial mode (*e.g.,* Latif & Grötzner, 2000). The 1-3 month leading, significant correlation of U_{WAtl} to Atl3 in June with a peak at one-month leading indicates that the equatorial oscillation is mostly excited by surface zonal wind anomalies in the western basin likely through oceanic dynamics (*e.g.,* Zebiak, 1993; Carton & Huang, 1994; Delecluse et al., 1994; Latif & Grötzner, 2000).

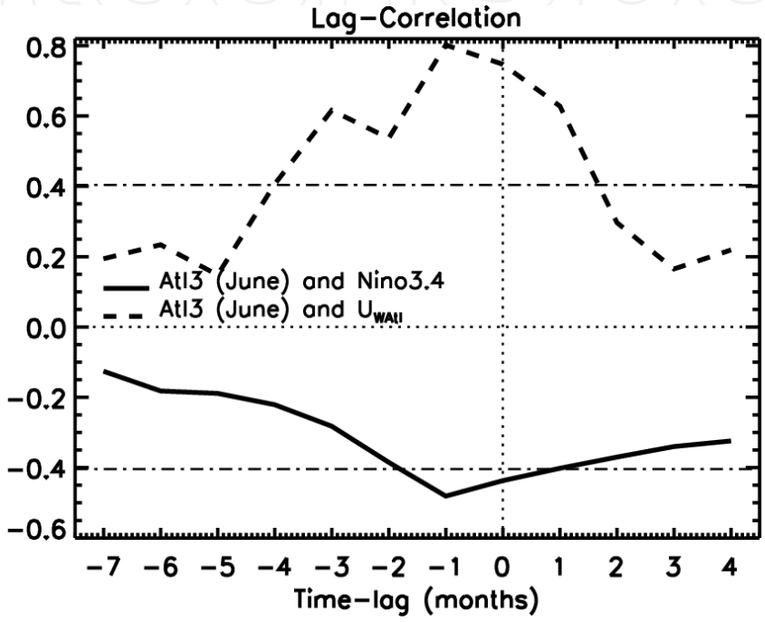

Fig. 6. Lag-correlations between Atl3 in June with Nino3.4 and U_{WAtl}, respectively. Positive (negative) months indicate Atl3 leads (lags) Nino3.4 and U_{WAtl}. The 5% significance level is ±0.42 based on 20 dofs.

The lag-correlation between U_{WAtl} in May and Nino3.4 is depicted in Fig. 7. The highest correlation appears as Nino3.4 leads U_{WAtl} by one-month, suggesting a strong impact from the equatorial Pacific (*e.g.,* Latif & Grötzner, 2000), and this impact probably being through anomalous Walker circulation and not passing through the mid-latitudes.

North of the equator, TNA and TNA1 both peak in April (Fig. 4). Simultaneous correlations between these two and Nino3.4 at the peak month are much weaker than when Nino3.4 leads them by at least one-month (Fig. 8). It is further noticed that the consistent high lag-correlations are seen with Nino3.4 leading by 1-7 months. Significant correlations of TNA and TNA1 in April with Nino3.4 can actually be found as Nino3.4 leads them up to 10 months (not shown). These highly consistent lag-relations suggest that the impact from the equatorial Pacific on the tropical north Atlantic may go through two ways: the Pacific-North-American (PNA) teleconnection and the anomalous Walker circulation (*e.g.,* Nobre & Shukla, 1996; Saravanan & Chang, 2000; Chiang et al., 2002), with the trade wind anomalies being the critical means. Most previous studies generally emphasized the first means being

available during boreal winter and spring (*e.g.*, Curtis & Hastenrath, 1995; Nobre & Shukla, 1996).

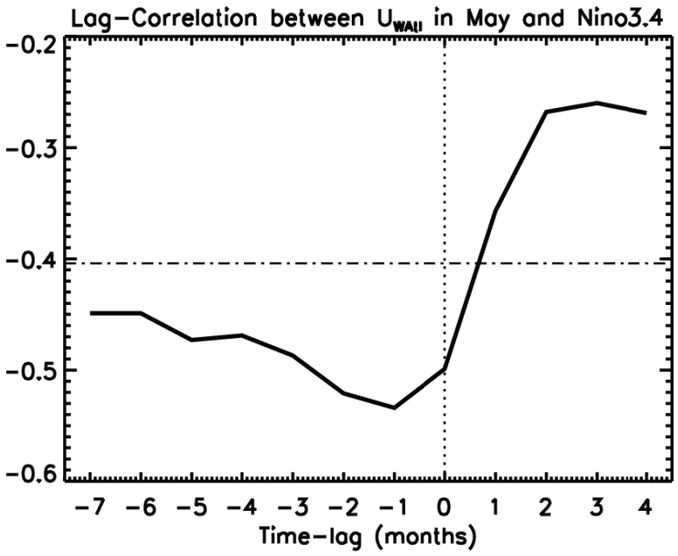

Fig. 7. Lag-correlation between U_{WAtl} in May with Nino3.4. Positive (negative) months indicate U_{WAtl} leads (lags) Nino3.4. The 5% significance level is ±0.42 based on 20 dofs.

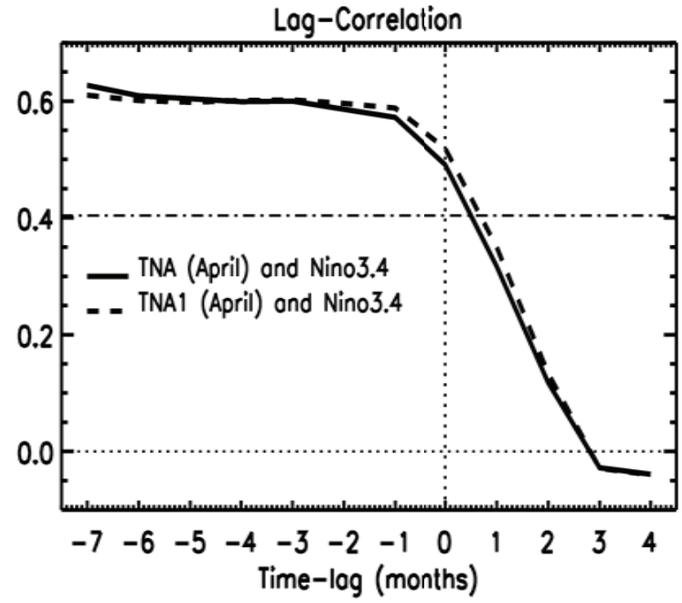

Fig. 8. Lag-correlations between TNA and TNA1 in April with Nino3.4. Positive (negative) months indicate TNA and TNA1 lead (lag) Nino3.4. The 5% significance level is ±0.42 based on 20 dofs.

4.2 Spatial structures of three SST modes related variations

Tables 1 and 2 illustrate the simultaneous correlations between the three SST indices (Atl3, TNA, and Nino3.4) and two rainfall indices (P_{ITCZ} and Lat_{ITCZ}). The ENSO events can effectively impact rainfall variability in the tropical Atlantic (*e.g.*, Nobre & Shukla, 1996;

Enfield & Mayer, 1997; Saravanan & Chang, 2000; Chiang et al., 2002; Giannini et al., 2004). A higher correlation (-0.62) can even be obtained between Nino3.4 and P_{dm}, implying a basin-wide impact in the equatorial region. The correlation between Nino3.4 and Lat_{ITCZ} is relatively weak during JJA, in contrasting to a much stronger impact during MAM.
Significant correlations appear between Atl3, and P_{ITCZ} and Lat_{ITCZ} during JJA and MAM (Tables 1 & 2). Even though the Atlantic equatorial warm/cold events are relatively weak and the ITCZ tends to be located about eight degrees north of the equator during boreal summer, the results suggest that the Atlantic Niño mode could still be a major factor controlling the ITCZ strength.
For the effect of TNA, large seasonal differences exist in its correlations with the rainfall indices (Tables 1 & 2). During JJA, TNA is significantly correlated with P_{ITCZ}. During MAM, however this correlation is much weaker. The correlation coefficient even changes sign between these two seasons. On the other hand, TNA is significantly correlated to Lat_{ITCZ} during MAM, but not during JJA.

γ	Nino3.4	Atl3	TNA
P_{ITCZ}	**-0.51**	**0.68**	**0.51**
Lat_{ITCZ}	0.39	**-0.65**	0.04

Table 1. Correlation coefficients (γ) between P_{ITCZ} (mm day^{-1}) and Lat_{ITCZ} (degree), and various SST indices during JJA. γ=±0.40 is the 5% significance level based on (n-2=) 23 dofs.

γ	Nino3.4	Atl3	TNA
P_{ITCZ}	**-0.50**	**0.56**	-0.18
Lat_{ITCZ}	**0.57**	**-0.67**	**0.41**

Table 2 Correlation coefficients (γ) between P_{ITCZ} (mm day^{-1}) and Lat_{ITCZ} (degree), and three SST indices during MAM. γ=±0.40 is the 5% significance level based on (n-2=) 23 dofs.

The modulations of the three major SST modes on the tropical Atlantic during JJA and MAM are further quantified by computing the regressions based on their seasonal-mean magnitudes normalized by their corresponding standard deviations.
Fig. 9 depicts the SST, surface wind, and precipitation associated with Atl3. During JJA, the spatial patterns generally agree with shown in previous studies that primarily focused on the peak months of the Atlantic equatorial mode (*e.g.*, Ruiz-Barradas et al., 2000; Wang, 2002). Basin-wide warming is seen with the maximum SSTs along the equator and tends to be in the eastern basin (Fig. 9b). Surface wind anomalies in general converge into the maximum, positive SST anomaly zone. Accompanying strong cross-equatorial flows being in the eastern equatorial region, anomalous westerlies are seen in the western basin extending from the equator to about 15°N. These wind anomalies are related to the equatorial warming (Figs. 5, 6), and also might be the major reason for the warming-up in the TNA/TNA1 region. Off the coast of West Africa, there even exist weak southerly anomalies between 10°-15°N. Positive rainfall anomalies are dominant in the entire basin, corresponding to the warm SSTs. It is interesting to note that these rainfall anomalies tend to be over the same area as the seasonal mean rainfall variances (Fig. 1). Particularly, over the open ocean the maximum rainfall anomaly band is roughly sandwiched by the marine ITCZ and the equatorial zone with maximum SST variability (Figs. 1c, 9b, and 9d), confirming the strong modulations of the equatorial mode during this season (Fig. 2). During MAM,

positive SST anomalies already appear along the equator (Fig. 9a). However, in addition to the SST anomalies along the equator, the most intense SST variability occurs right off the west coast of Central Africa, reflecting the frequent appearance of the Benguela Niño peaking in March-April (*e.g.,* Florenchie et al., 2004). North of the equator, negative SST anomalies, though very weak, can still be seen off the West African coast. This suggests that the Atlantic Niño may effectively contribute to the interhemispheric SST mode peaking in this season, particularly to its south lobe (Figs. 1b and 9a). Negative-positive rainfall anomalies across the equator forming a dipolar structure are evident, specifically west of 20°W (Fig. 9c). In the Gulf of Guinea, positive rainfall anomalies, though much weaker than in the western basin, can still be observed extending from the open ocean to the west coast of Central Africa, roughly following strong positive SST anomalies.

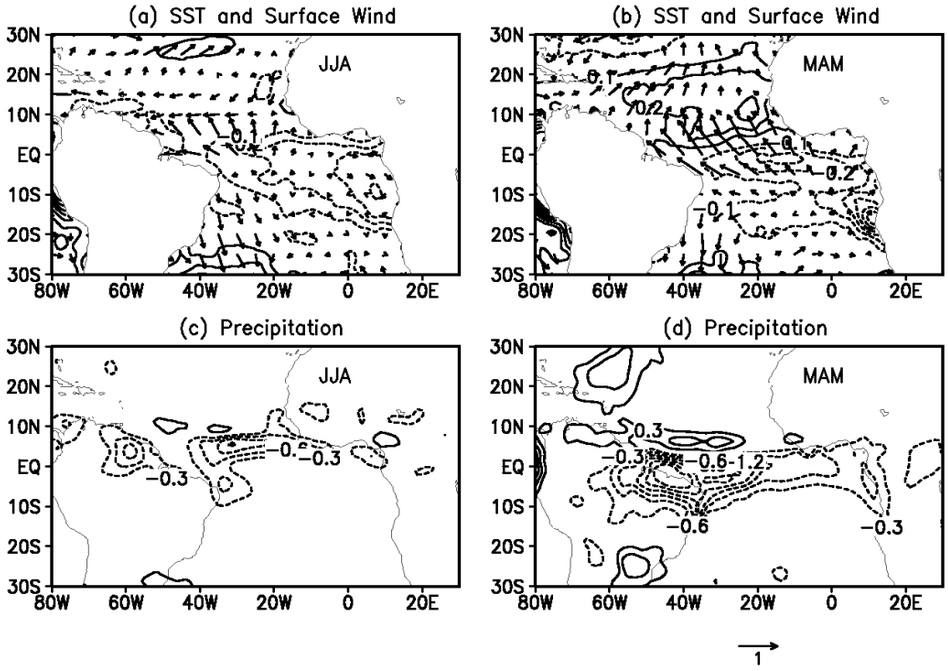

Fig. 9. Regression onto Nino3.4 of SST and surface wind (a, b), and precipitation (c, d) anomalies during JJA (a, c) and MAM (b, d).

The SST, surface wind, and rainfall anomalies associated with TNA are shown in Fig. 10. Positive SST anomalies appear north of the equator during MAM, but become weaker during JJA. Surface wind vectors converge into the warm SST region, resulting in the decrease in the mean trade winds north of the equator. Cross-equatorial flow is strong during MAM, implying TNA's contribution to the interhemispheric SST mode. On the other hand, no evident SST anomalies appear along and south of the equator supporting that the two lobes of the interhemispheric mode are probably not connected (*e.g.,* Enfield et al., 1999). A negative-positive rainfall dipolar feature occurs during MAM with much weaker anomalies east of 20°W, consistent with previous studies (*e.g.,* Nobre & Shukla, 1996; Ruiz-Barradas et al., 2000; Chiang et al., 2002). During JJA, however only appears a single band of positive rainfall anomalies between 5°-20°N, covering the northern portion of the mean rainfall within the ITCZ and its variances (Figs. 1c, 1d, and 10d). Interestingly this band tilts

from northwest to southeast, tending to be roughly along the tracks of tropical storms. This may reflect the impact of TNA on the Atlantic hurricane activity (*e.g.*, Xie et al., 2005).

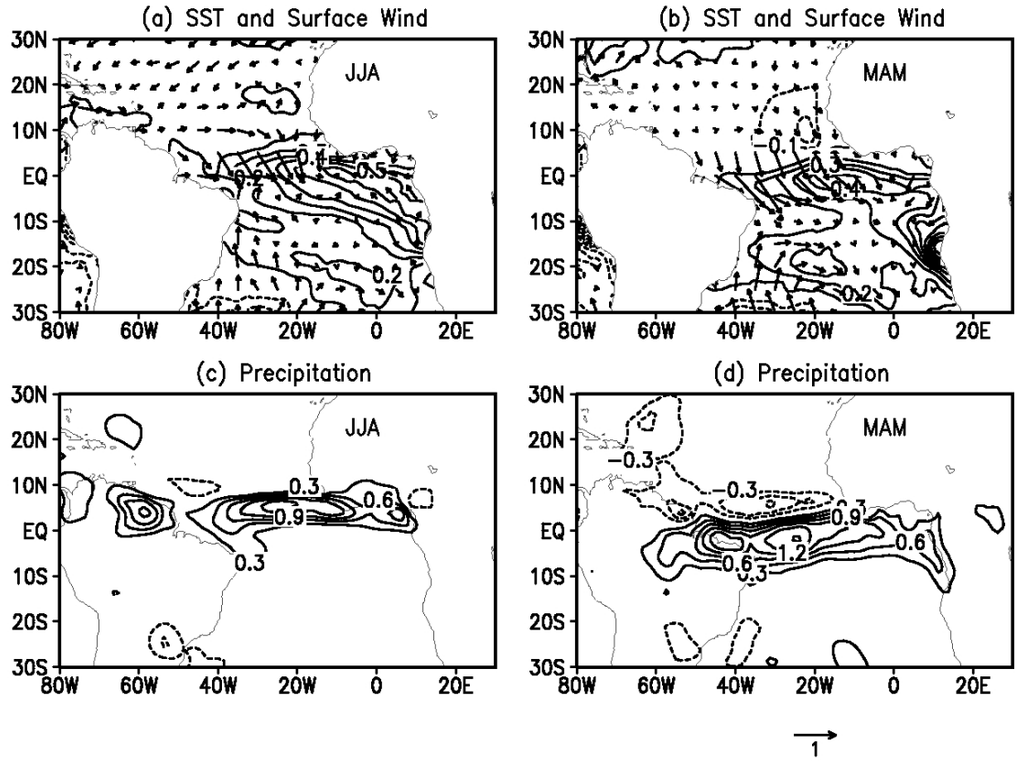

Fig. 10. Regression onto Atl3 of SST and surface wind (a, b), and precipitation (c, d) anomalies during JJA (a, c) and MAM (b, d).

Fig. 11 illustrates the SST, surface wind, and rainfall regressed onto the seasonal mean Nino3.4. During MAM, positive-negative SST anomalies occur in the tropical region, shaping a dipolar structure accompanied by strong cross-equatorial surface winds. Compared with Figs. 9a and 10a, it is likely that ENSO may contribute to both lobes of the interhemispheric SST mode during this season (*e.g.*, Chiang et al., 2002). Rainfall anomalies tend to be in the western basin and manifest as dipolar as well. Compared with Figs. 9a and 9c, it is noticeable that along and south of the equator, ENSO shows a very similar impact feature as the Atlantic equatorial mode except with the opposite sign. This enhances our discussion about their relations (Figs. 5 and 6). During JJA, SST anomalies almost disappear north of the equator. South of the equator, negative SST anomalies can still be seen but become weaker, accompanied by much weaker equatorial wind anomalies. Rainfall anomalies move to the north, as does the ITCZ. The dipolar feature can hardly be discernible. Again, the rainfall anomalies show a very similar pattern as those related to Atl3 (Figs. 9d and 11d), though their signs are opposite. This seems to suggest that during JJA the impact of ENSO on the tropical Atlantic may mostly go through its influence on the Atlantic equatorial mode (Atl3).

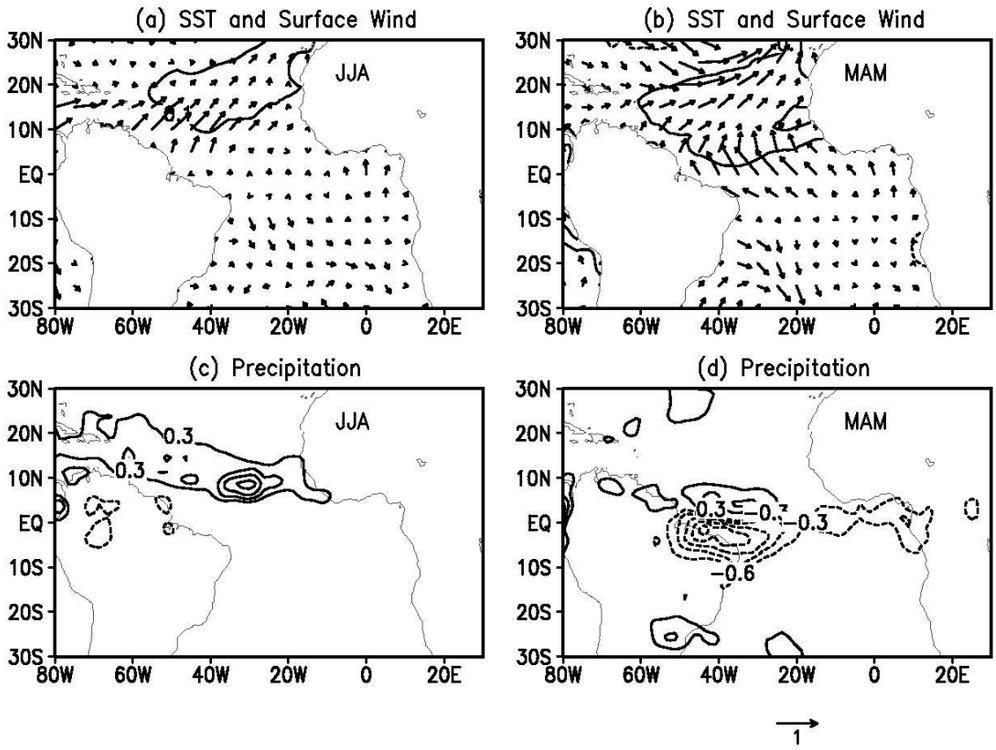

Fig. 11. Regression onto TNA of SST and surface wind (a, b), and precipitation (c, d) anomalies during JJA (a, c) and MAM (b, d).

Therefore, generally consistent with past results (e.g., Nobre & Shukla, 1996; Enfield & Mayer, 1997; Saravanan & Chang, 2000; Chiang et al., 2002; Giannini *et al.* 2004), these three SST modes all seem to influence rainfall variations in the tropical Atlantic, though through differing means. However, strong inter-correlations have been shown above among these SST indices and in past studies (e.g., Münnich & Neelin, 2005; Gu & Adler, 2006). Nino3.4 is significantly correlated with Atl3 during both JJA (-0.46) and MAM (-0.53), and with TNA (0.52) during MAM. Previous studies have demonstrated that the Pacific ENSO can modulate SST in the tropical Atlantic through both mid-latitudes and anomalous Walker circulation (e.g., Horel & Wallace, 1981; Chiang et al., 2002; Chiang & Sobel, 2002). While no significant correlation between Nino3.4 and Atl3 was found in some previous studies (e.g., Enfield & Mayer, 1997), high correlations shown here are generally in agreement with others (e.g., Delecluse et al., 1994; Latif & Grötzner, 2000). Thus, the correlations shown above, particularly the effect of Nino3.4, may be complicated by the inter-correlations among the SST indices. For instance, the high correlation between Nino3.4 and P_{ITCZ} may primarily result from their respective high correlations with Atl3 (Tables 1 & 2), and hence may not actually indicate any effective, direct modulation of convection (P_{ITCZ}) by the ENSO. It is thus necessary to discriminate their effects from each other. Thus, linear correlations and second-order partial correlations are estimated and further compared (Figs. 12 and 13). The second-order correlation here represents the linear correlation between rainfall and one SST index with the effects of other two SST indices removed (or hold constant) (Gu &Adler, 2009). With or without the effects of Nino3.4 and TNA, the spatial structures of correlation with Atl3 do not vary much. With the impact of Nino3.4 and TNA removed, the Atl3 effect

only becomes slightly weaker during both JJA and MAM. Given a weak relationship between Atl3 and TNA (0.17 during JJA and -0.16 during MAM; Enfield et al., 1999), this correlation change is in general due to the Pacific ENSO.

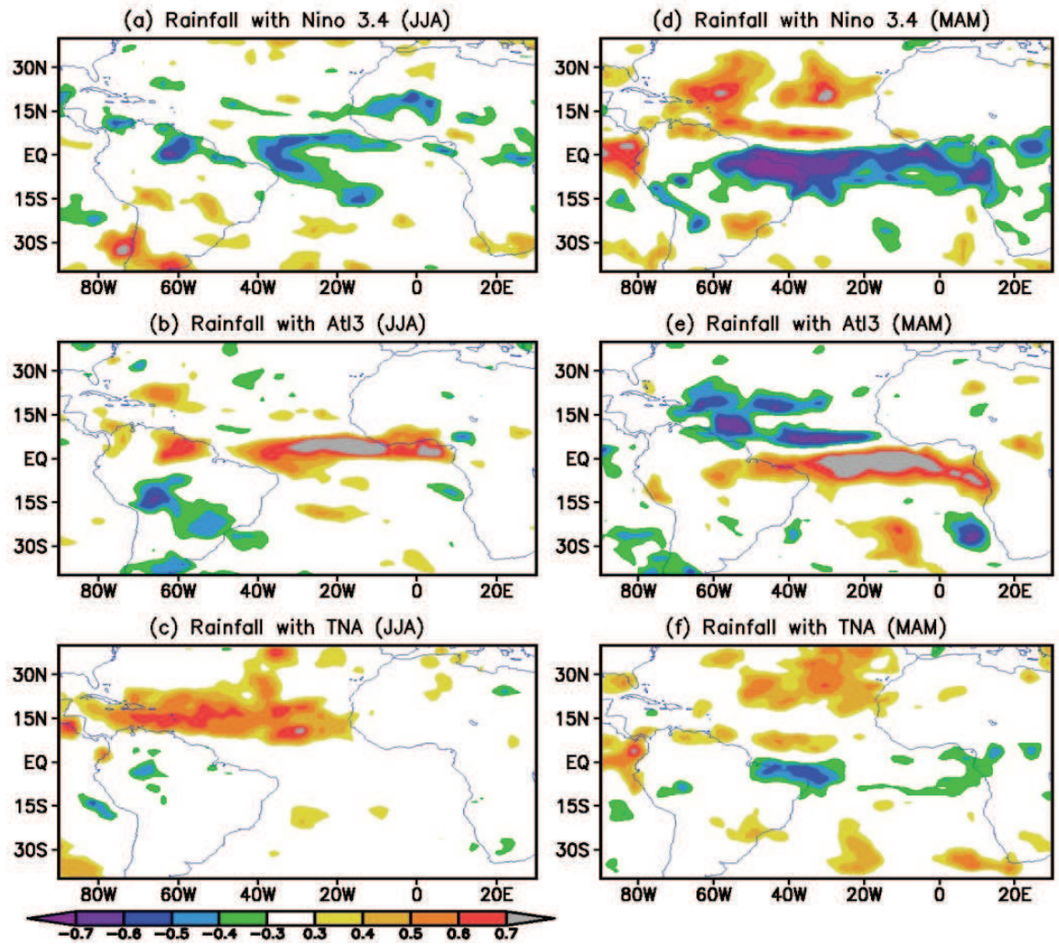

Fig. 12. Correlation maps of seasonal-mean rainfall anomalies in the tropical Atlantic with (a, d) Nino3.4, (b, e) Atl3, and (c, f) TNA during JJA (left) and MAM (right). The 5% significance level is ±0.4 based on 23 dofs.

During JJA, Nino3.4 and Atl3 have very limited impact on the TNA associated rainfall anomalies, likely due to TNA's weak correlation with both Nino3.4 (-0.06) and Atl3 (0.17). The second-order partial correlation between TNA and P_{ITCZ} slightly increases to 0.57. This high correlation coefficient seems to be reasonable because the marine ITCZ is then directly over the tropical North Atlantic (Fig. 1). During MAM, the effect of TNA on rainfall over the tropical open ocean is generally weak. With the effects of Nino3.4 and Atl3 removed, the large area of negative correlation in the western basin near South America shrinks into a much smaller region.

Hence, the direct influence of ENSO through the anomalous Walker circulations could play a role, but in general is confined in the western basin and over the northeastern South American continent where the most intense deep convection and variations are located

during MAM (Fig. 1). During JJA, this kind of modulation of deep convection disappears because the ITCZ moves to the north and stays away from the equator. The ENSO impact on rainfall anomalies in the tropical Atlantic may hence primarily go through its effect on the two local SST modes. In particular, its effect on Atl3 seems to be the only means during JJA by means of modulating surface winds in the western basin (Figs. 6 and 7; e.g., Latif & Grötzner, 2000; Münnich & Neelin, 2005). These wind anomalies are essential components for the development of the Atlantic Niño mode (e.g., Zebiak, 1993; Latif & Grötzner, 2000).

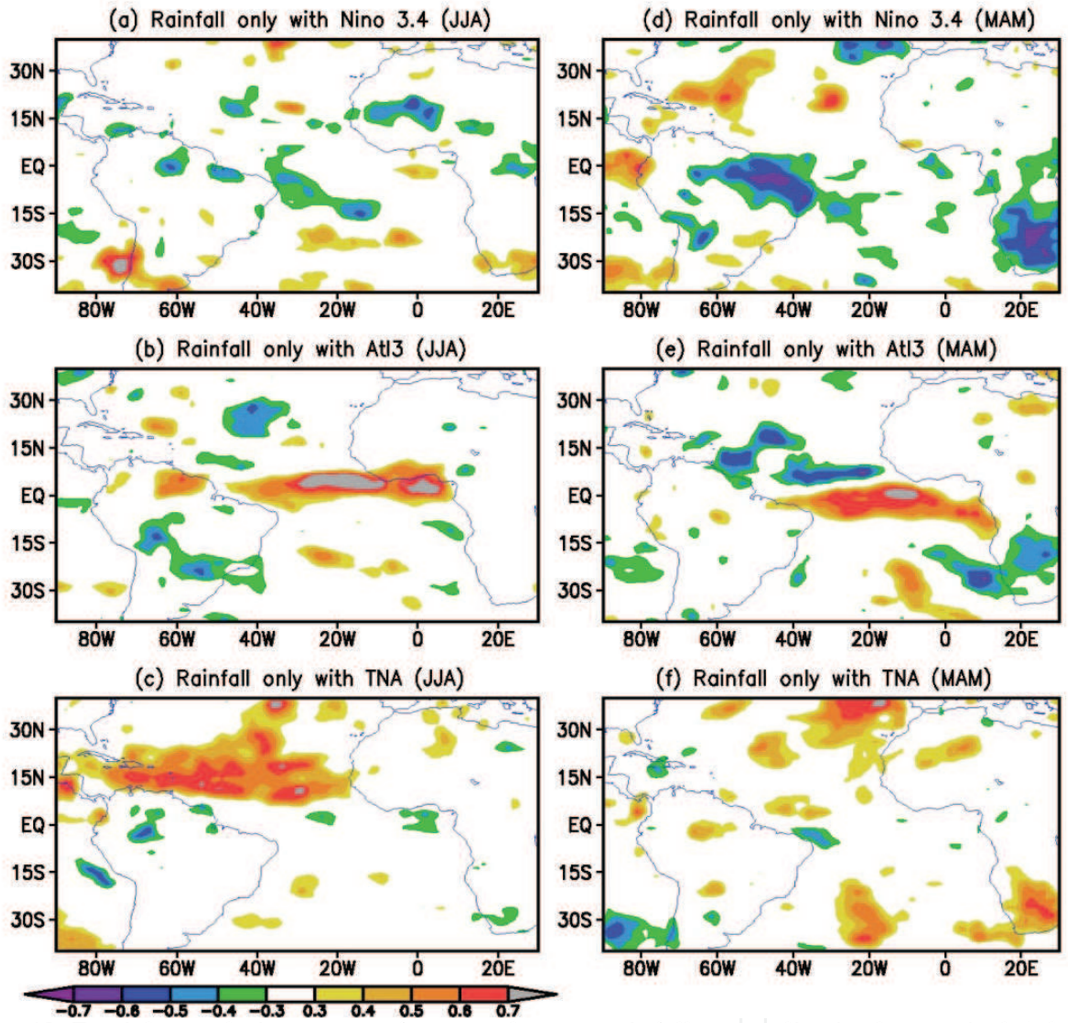

Fig. 13. Partial-correlation maps of seasonal-mean rainfall anomalies in the tropical Atlantic with (a, d) Nino3.4, (b, e) Atl3, and (c, f) TNA during JJA (left) and MAM (right). The second-order partial correlations are estimated by limiting the effects of any two other indices. The 5% significance level is ±0.41 based on 21 dofs.

5. Summary and conclusions

Seasonal-mean rainfall in the tropical Atlantic during JJA shows intense interannual variabilities, which are comparable with during MAM based on both the ITCZ strength and the basin-mean rainfall. The latitudes of the marine ITCZ however do not vary much from-

year-to-year during JJA, in contrasting to evident variations occurring during MAM. Hence the summer-time rainfall variability is mostly manifested as the variations in the ITCZ strength and the basin-mean rainfall.

Rainfall variations associated with the two local SST modes and ENSO are further examined. The Atlantic Niño mode can effectively induce rainfall anomalies during JJA through accompanying anomalous surface winds and SST. These rainfall anomalies are generally located over the major area of rainfall variance. TNA can contribute to the rainfall changes as well during this season, but its impact is mostly limited to the northern portion of the ITCZ. The ENSO teleconnection mechanism may still play a role during boreal summer, although it becomes much weaker than during boreal spring. It is noticed that the ENSO-associated spatial patterns tend to be similar to those related to the Atlantic Niño though with an opposite sign. This suggests that the impact of ENSO during JJA may go through its influence on the Atlantic Niño mode.

During MAM, TNA shows an evident impact on rainfall changes specifically in the region near and over the northeastern South America. The correlation/regression patterns are generally consistent with those using the index representing the interhemispheric SST mode (*e.g.,* Ruiz-Barradas et al., 2000), though the TNA-associated SST anomalies are weak and mostly north of the equator. This suggests a strong contribution of TNA to this interhemispheric mode and also its independence from the SST oscillations south of the equator (*e.g.,* Enfield et al., 1999). Atl3 and Nino3.4 can contribute to the interhemispheric SST mode too, in addition to their direct modulations of rainfall change in the basin. Particularly in the western basin (west of 20^{o}W), corresponding to evident oscillations of the ITCZ locations, a dipolar feature of rainfall anomalies occurs in the regression maps for both indices. Simultaneously appear strong surface wind anomalies with evident cross-equatorial components.

To further explore the relationships among the two local SST modes and ENSO, contemporaneous and lag correlations are estimated among various indices. ENSO shows strong impact on the Atlantic equatorial region and the tropical north Atlantic. Significant, simultaneous correlations between Nino3.4 and TNA are seen during February-April. Significant lag-correlation of TNA at its peak month (April) with Nino3.4 one or several months before further confirms that the impact from the tropical Pacific is a major contributor during boreal spring (*e.g.,* Chiang et al., 2000). Nino3.4 is highly correlated with Atl3 during April-June. The correlations between Nino3.4 and zonal wind index in the west basin (U_{Watl}) also become high during April-July. Moreover the maximum correlation between U_{Watl} in May (peak month) and Nino3.4 is seen as Nino3.4 precedes it by one month, indicating the remote modulations of wind anomalies. The Pacific ENSO can effectively modulate convection and surface winds during boreal spring through both ways: the PNA and the anomalous Walker cell (*e.g.,* Nobre & Shukla, 1996; Chiang & Sobel, 2002). Trade wind anomalies are a pathway for the SST oscillations north of the equator (*e. g.,* Curtis & Hastenrath, 1995; Enfield & Mayer, 1997). Along and south of the equator, convective and wind anomalies in the western basin are the critical means for the ENSO impact. During JJA, the pathway from the mid-latitudes becomes impossible due to seasonal changes in the large-scale mean flows, and the ITCZ moves away from the equator. Hence, the ENSO impact on the tropical region is greatly limited. The lag-correlations between Atl3 at the peak month (June) and Nino3.4 and U_{Watl}, respectively, tend to suggest that the equatorial oscillation is excited by the preceding surface wind anomalies in the west basin

that are closely related to the ENSO. The lag and simultaneous correlations of Atl3 with U_{Watl} further confirm that it is a coupled mode to a certain extent. It is interesting to further note that high positive correlations can be found between Atl3 and TNA/TNA1 during July-October, implying that during JJA the Atlantic equatorial mode may have a much more comprehensive impact, in addition to its influence on the ITCZ, than expected.

A second-order partial correlation analysis is further applied to discriminate the effects of these three SST modes because of the existence of inter-correlations among them. With the effects of Atl3 and TNA removed, ENSO only has a very limited direct impact on the open ocean in the tropical Atlantic, and its impact is generally confined in the western basin and over the northeastern South America.

Therefore, during JJA, the two local SST modes turn out to be more critical/essential for rainfall variations in the tropical Atlantic. The effect of the Pacific ENSO on the tropical Atlantic is in general through influencing the Atlantic Niño mode, and surface zonal wind anomalies in the western basin are the viable means to realize this effect.

6. References

Adler, R.; & Coauthors (2003). The version 2 Global Precipitation Climatology Project (GPCP) monthly precipitation analysis (1979-present). *J. Hydrometeor*, **4**, 1147-1167.

Biasutti, M.; Battisti, D. & Sarachik, E. (2004). Mechanisms controlling the annual cycle of precipitation in the tropical Atlantic sector in an atmospheric GCM. *J. Climate*, **17**, 4708-4723.

Carton, J. & Huang, B. (1994). Warm events in the tropical Atlantic. *J. Phys. Oceanogr.,* **24**, 888-903.

Chen, Y. & Ogura, Y. (1982). Modulation of convective activity by large-scale flow patterns observed in GATE. *J. Atmos. Sci.,* **39**, 1260-1279.

Chiang, J.; Kushnir, Y. & Zebiak, S. (2000). Interdecadal changes in eastern Pacific ITCZ variability and its influence on the Atlantic ITCZ. *Geophys. Res. Lett.*, **27**, 3687-3690.

Chiang, J.; Kushnir, Y. & Giannini, A. (2002). Reconstructing Atlantic Intertropical Convergence Zone variability: Influence of the local cross-equatorial sea surface temperature gradient and remote forcing from the eastern equatorial Pacific. *J. Geophys. Res.*, **107**(D1), 4004, doi:10.1029/2000JD000307.

Chiang, J. & Sobel, A. (2002). Tropical tropospheric temperature variations caused by ENSO and their influence on the remote tropical climate. *J. Climate*, **15**, 2616-2631.

Curtis, S. & Hastenrath, S. (1995). Forcing of anomalous sea surface temperature evolution in the tropical Atlantic during Pacific warm events. *J. Geophys. Res.*, **100**, 15835-15847.

Czaja, A. (2004). Why is North Tropical Atlantic SST variability stronger in boreal spring? *J. Climate*, **17**, 3017-3025.

Delecluse, P.; Servain, J., Levy, C., Arpe, K. & Bengtsson, L. (1994). On the connection between the 1984 Atlantic warm event and the 1982-1983 ENSO. *Tellus*, **46**A, 448-464.

Enfield, D. & Mayer, D. (1997). Tropical Atlantic sea surface temperature variability and its relation to El Niño-Southern Oscillation. *J. Geophys. Res.,* **102**, 929-945

Enfield, D.; Mestas-Nunez, A., Mayer, D. & and Cid-Serrano, L. (1999). How ubiquitous is the dipole relationship in tropical Atlantic sea surface temperature? *J. Geophys. Res.*, **104**, 7841-7848.

Florenchie, P.; Reason, C., Lutjeharms, J., Rouault, M., Roy, C. & Masson, S. (2004). Evolution of interannual warm and cold events in the southeast Atlantic Ocean. *J. Climate*, **17**, 2318-2334.

Giannini, A.; Chiang, J., Cane, M., Kushnir, Y. & Seager, R. (2001). The ENSO teleconnection to the tropical Atlantic Ocean: Contributions of the remote and local SSTs to rainfall variability in the tropical Americas. *J. Climate*, **14**, 4530-4544.

Giannini, A.; Saravanan, R. & Chang, P. (2004). The preconditioning role of tropical Atlantic variability in the development of the ENSO teleconnection: Implication for the predictability of Nordeste rainfall. *Climate Dyn.,* **22**, 839-855.

Gill, A. (1982). *Atmosphere-Ocean Dynamics*. Academic Press, 662pp.

Gu, G., & Adler, R. (2004). Seasonal evolution and variability associated with the West African monsoon system. *J. Climate*, **17**, 3364-3377.

Gu, G. & Adler, R. (2006). Interannual rainfall variability in the tropical Atlantic region. *J. Geophys. Res.,* **111**, D02106, doi:10.1029/2005JD005944.

Gu, G. & Adler, R. (2009). Interannual Variability of Boreal Summer Rainfall in the Equatorial Atlantic. *Int. J. Climatol.,* **29**, 175-184, doi: 10.1002/joc.1724.

Gu, G. & Zhang, C. (2001). A spectrum analysis of synoptic-scale disturbances in the ITCZ. *J. Climate*, **14**, 2725-2739.

Hastenrath, S. & Greischar, L. (1993). Circulation mechanisms related to northeast Brazil rainfall anomalies. *J. Geophys. Res.,* **98**, 5093-5102.

Kalnay, E.; & Coauthors (1996). The NCEP/NCAR 40-year reanalysis project. *Bull. Amer. Meteor. Soc.*, **77**, 437-471.

Lamb, P. (1978a). Large scale tropical Atlantic surface circulation patterns during recent sub-Saharan weather anomalies. *Tellus*, **30**, 240-251.

Lamb, P. (1978b). Case studies of tropical Atlantic surface circulation patterns during recent sub-Saharan weather anomalies: 1967 and 1978. *Mon. Wea. Rev.,* **106**, 482-491.

Landsea, C.; Pielke Jr., R., Mesta-Nunez, A. & Knaff, J. (1999). Atlantic basin hurricanes: Indices of climate changes. *Climate Change*, **42**, 89-129.

Latif, M. & Grötzner, A. (2000). The equatorial Atlantic oscillation and its response to ENSO. *Climate Dyn.,* **16**, 213-218.

Mitchell, T. & Wallace, J. (1992). The annual cycle in equatorial convection and sea surface temperature. *J. Climate*, **5**, 1140-1156.

Münnich, M. & Neelin, J. (2005). Seasonal influence of ENSO on the Atlantic ITCZ and equatorial South America. *Geophys. Res. Lett.,* **32**, L21709, doi:10.1029/2005GL023900.

Nobre, P. & Shukla, J. (1996). Variations of sea surface temperature, wind stress, and rainfall over the tropical Atlantic and South America. *J. Climate*, **9**, 2464-2479.

Reynolds, R.; Rayner, N., Smith, T., Stokes, D. & and Wang, W. (2002). An improved in situ and satellite SST analysis for climate. *J. Climate*, **15**, 1609-1625.

Ruiz-Barradas, A.; Carton, J. & Nigam, S. (2000). Structure of interannual-to-decadal climate variability in the tropical Atlantic sector. *J. Climate*, **13**, 3285-3297.

Saravanan, R. & Chang, P. (2000). Interaction between tropical Atlantic variability and El Niño-Southern oscillation. *J. Climate*, **13**, 2177-2194.

Sutton, R.; Jewson, S. & Rowell, D. (2000). The elements of climate variability in the tropical Atlantic region. *J. Climate*, **13**, 3261-3284.

Thorncroft, C. & Rowell, D. (1998). Interannual variability of African wave activity in a general circulation model. *Int. J. Climatol.*, **18**, 1306-1323.

Wang, C. (2002). Atlantic climate variability and its associated atmospheric circulation cells. *J. Climate*, **15**, 1516-1536.

Xie, L.; Yan, T. & Pietrafesa, L. (2005). The effect of Atlantic sea surface temperature dipole mode on hurricanes: Implications for the 2004 Atlantic hurricane season. *Geophys. Res. Lett.*, **32**, L03701, doi:10.1029/2004GL021702.

Zebiak, S. (1993). Air-sea interaction in the equatorial Atlantic region. *J. Climate*, **6**, 1567-1586.

IntechOpen

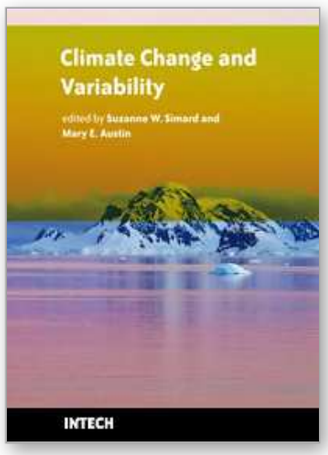

Climate Change and Variability

Edited by Suzanne Simard

ISBN 978-953-307-144-2

Hard cover, 486 pages

Publisher Sciyo

Published online 17, August, 2010

Published in print edition August, 2010

Climate change is emerging as one of the most important issues of our time, with the potential to cause profound cascading effects on ecosystems and society. However, these effects are poorly understood and our projections for climate change trends and effects have thus far proven to be inaccurate. In this collection of 24 chapters, we present a cross-section of some of the most challenging issues related to oceans, lakes, forests, and agricultural systems under a changing climate. The authors present evidence for changes and variability in climatic and atmospheric conditions, investigate some the impacts that climate change is having on the Earth's ecological and social systems, and provide novel ideas, advances and applications for mitigation and adaptation of our socio-ecological systems to climate change. Difficult questions are asked. What have been some of the impacts of climate change on our natural and managed ecosystems? How do we manage for resilient socio-ecological systems? How do we predict the future? What are relevant climatic change and management scenarios? How can we shape management regimes to increase our adaptive capacity to climate change? These themes are visited across broad spatial and temporal scales, touch on important and relevant ecological patterns and processes, and represent broad geographic regions, from the tropics, to temperate and boreal regions, to the Arctic.

IntechOpen